Received: 18 October 2021 | Revised: 30 May 2022 | Accepted: 13 June 2022

IET Generation, Transmission & Distribution

DOI: 10.1049/gtd2.12547

The Institution of Engineering and Technology WILEY

ORIGINAL RESEARCH

Static and dynamic eigenvalues in unified stability studies

Jalal Khodaparast[1] | **Olav Bjarte Fosso**[2] | **Marta Molinas**[3] | **Jon Are Suul**[3,4]

[1]Department of Electrical Engineering, IT and Cybernetic, University of South-Eastern Norway (USN), Porsgrunn, Norway

[2]Department of Electric Power Engineering, Norwegian University of Science and Technology (NTNU), Trondheim, Norway

[3]Department of Engineering Cybernetics, Norwegian University of Science and Technology (NTNU), Trondheim, Norway

[4]Department of Energy Systems, SINTEF Energy Research, Trondheim, Norway

Correspondence
Jalal Khodaparast, University of South-Eastern Norway (USN), Porsgrunn, Norway.
Email: jalal.khodaparast@usn.no

[Correction added on 9-July-2022, after first online publication: Author affiliations have been updated in this version].

Abstract

A framework for unified analysis of small-signal and large-signal power system stability based on static and dynamic eigenvalues is proposed in this paper. The presented implementation is based on Gear's method, which is a two-step integration method for numerical simulation with self-adaptive time-step. Furthermore, it can be easily configured for providing the state matrix as basis for calculating the system eigenvalues during simulation. Thus, the presented framework allows for eigenvalue-based analysis of small-signal dynamics and stability margin at any steady-state operating point during a time-domain simulation. Furthermore, Linear Time-Varying system theory is utilized for modal analysis during large-signal transients. For this purpose, dynamic eigenvalues and eigenvectors are calculated by solving a Riccati equation to generalize the modal analysis during transient conditions. The stability is evaluated by calculating the Lyapunov exponent of the mode-vector of the system. The results from numerical analysis of three case studies are presented to evaluate and illustrate the characteristics of the presented approach for unified small-signal and transient stability analysis.

1 | INTRODUCTION

Large-scale introduction of converter-interfaced Renewable Energy Sources (RESs), High Voltage Direct Current (HVDC) transmission and Flexible AC Transmission Systems (FACTSs) is increasing the complexity of power systems. Therefore, stability analysis will become more demanding [1, 2]. In particular, power electronic components and their control loops can experience interactions with conventional power system elements, which make the stability analysis more challenging than for conventional systems dominated by synchronous machines[3]. In this emerging context of modern AC/DC power systems, multiple components exhibit a wide range of time constants in their dynamic response. Accordingly, improved techniques and new tools should be adopted to accurately and efficiently analyze the stability of modern power systems [4, 5].

In general terms, power system stability refers to the ability of an electric power system to recover an equilibrium point with system variables bounded after being subjected to a disturbance. Different categories of stability have been defined and partly changed over time, but the definition of rotor angle stability has been unaffected [6, 7]. It refers to the ability of synchronous machines to remain in synchronism after being subjected to a disturbance. Rotor angle stability is categorized in terms of two subcategories: Small-disturbance (or small-signal) and large-disturbance (transient) rotor angle stability. Indeed, many methods in the literature deal with stability analysis from both point of views.

Small-signal stability analysis is based on linearizing the nonlinear system around an operating point and subsequent application of linear analysis [8]. The analysis can be based on different methods such as: transfer function (closed/open loop, single/multi-input and single/multi-output) [9], eigenvalue extraction from the state-space model of the system[10], and impedance-based analysis using Nyquist theorem[10]. On the other hand, large-signal stability analysis examines the power system under nonlinear conditions. Lyapunov-based methods are direct methods that examine the stability of a power system without solving the differential equations [11–13]. However, obtaining an appropriate Lyapunov function is very complicated in a large-scale power system. Therefore, time-domain simulation by numerical integration methods is currently the most widely used approach for transient stability analysis. Differential and algebraic equations of the power system are then solved by a numerical method, and transient indices are derived from the resulting time-domain response [14].

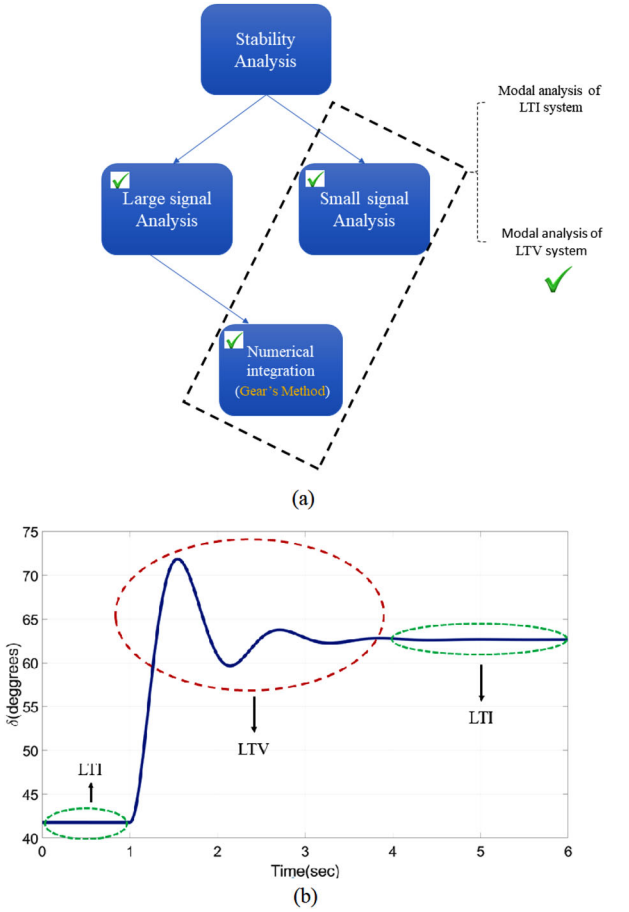

FIGURE 1 Contribution of the proposed method in a stability analysis, a) field of study of the proposed method, b) Switching between LTI and LTV in the proposed method

Gear's method as a second-order predictor-corrector method is a stiff solver, which performs the integration operation efficiently by adapting the step size automatically [15]. Implementing variable-time step simulation of hybrid *dq* and phasor models using Gear's method has advantages compared to methods implemented in the stationary frame. In this paper, we are utilizing Gear's method as a basis for developing a numerical algorithm for power system simulation that can simultaneously evaluate small and large-signal stability. The background for the choice of numerical method is that: 1) It is an adaptive step size algorithm, so it solves the challenge of large and complex power systems.[16]; and 2) According to the internal processes of the algorithm, it can be easily adapted for calculating indices of both small- and large-signal stability.

The main contribution of this paper is the introduction of a framework for combining small- and large-signal stability analysis. This can avoid the need for evaluating non-linear and linearized system models individually by using different tools for the stability analysis. It is proposed to use the A-matrix as a side-product of the Gear's method in a procedure to detect new information about the dynamic behavior of the simulated power system. As shown in Figure 1a, the proposed method arises from the connection of the numerical integration method and modal analysis.

Consider as an example the generic time-domain response of a generator shown in Figure 1b, in which the system is in steady-state condition before time = 1 s. During steady-state conditions, the method can extract the state matrix (A) of the system, to evaluate the system's stability margin by monitoring the critical static eigenvalue (it is called "static" in this paper because it is constant). However, the system is subjected to a disturbance at time = 1 s and responds with a transient response. During the transient condition (1 s $< t <$ 4 s), the extracted A-matrix of the stressed system will be time-varying, for which the Linear Time-Varying (LTV) system theory is applicable. Finally, after the transient behavior settles down (4 s $< t <$ 6 s), the small-signal dynamics can again be analyzed by tools for LTI systems. In this paper, a unified method is proposed to perform modal analysis both during steady-state and dynamic conditions. It is worth noting that the assessment must be switched from LTI to LTV and vice versa in Figure 1b. In the proposed method, changes in he A-matrix is the indicator utilised for switching between the two methods. If all elements of A-matrix will be unchanged in successive time steps, the system is in a steady-state condition, and LTI theory is applied. When one array changes, the LTV theory will be applied.

The presented methods are inspired from the general idea of unified small- and large-signal analysis introduced in [17]. However, the concept is further enriched by introducing LTV system analysis for assessing the transient stability by calculation of dynamic eigenvalues, dynamic eigenvectors and a Lyapunov exponent. The features of the proposed method are evaluated by analysis of three examples including a multi-machine power system with an HVDC interconnection. The proposed method can provide the following advantages:

- Unified analysis of small-signal and large-signal stability by providing the possibility for small-signal stability analysis as a part of an algorithm for numerical time-domain simulation. Therefore, it is not necessary to evaluate the linear and nonlinear models individually by different tools for stability analysis.
- Systematic extraction of the "A"-matrix during time-domain simulation as a basis for conventional small-signal analysis by methods for LTI systems during steady-state conditions, and for analysis of LTV systems during transient conditions.
- Evaluation of the extracted LTV system and its corresponding dynamic eigenvalues and dynamic eigenvectors. This allows for large signal instability detection by analysis of the Lyapunov exponent in a unified framework for stability analysis.

The rest of the paper will first give an overview of the applied method for numerical simulation before introducing the concept of dynamic eigenvalues and eigenvectors and how this may be used to detect stability issues along the simulation trajectory. Discussion of implementation details are included to document how the applied method handles discrete events like disturbances and the nonlinearity imposed by limiters in control

systems. Furthermore, results from three case studies of different complexity are included to demonstrate the performance of the proposed concept.

2 | GEAR'S METHOD

Gear's method is a second-order numerical integration method that operates on prediction and correction stages. It can adjusts the integration step size based on the equations' instantaneous stiffness to fulfill the desired accuracy. It uses second-order Taylor expansion to predict the variables in the prediction stage and applies the Newton-Raphson method to correct the predictions in the correction stage[15, 18].

For defining the implementation of Gear's method we consider a general nonlinear Differential-Algebraic Equation (DAE) on the form of

$$\begin{aligned} y' &= f(y, x, t) \\ 0 &= g(y, x, t) \end{aligned} \tag{1}$$

where y is state variable, x is algebraic variable, f and g are nonlinear functions and t is time. In the prediction stage of Gear's method, the next step solution (y^P_{n+1}, x^P_{n+1}) and the first and second derivatives are predicted by the Taylor expansion as: [19]

$$y^P_{n+1} = y_n + H_{n+1} y'_n + H^2_{n+1} y''_n/2, \tag{2}$$

$$y'^P_{n+1} = y'_n + H_{n+1} y''_n, \tag{3}$$

$$y''^P_{n+1} = y''_n, \tag{4}$$

$$x^P_{n+1} = x_n + H_{n+1}\, x'_n + H^2_{n+1}\, x''_n/2, \tag{5}$$

$$x'^P_{n+1} = x'_n + H_{n+1}\, x''_n, \tag{6}$$

$$x''^P_{n+1} = x''_n, \tag{7}$$

where H is the integral step size, y', x', and y'', x'' are first and second derivatives. In the correction stage of Gear's method, the predicted values are corrected as:

$$y_{n+1} = y^P_{n+1} + \Delta y, \tag{8}$$

$$y'_{n+1} = y'^P_{n+1} + \Delta y\, I_1/H_{n+1}, \tag{9}$$

$$y''_{n+1} = y''^P_{n+1} + 2\Delta y\, I_2/H^2_{n+1}, \tag{10}$$

$$x_{n+1} = x^P_{n+1} + \Delta x, \tag{11}$$

$$x'_{n+1} = x'^P_{n+1} + \Delta x\, I_1/H_{n+1}, \tag{12}$$

$$x''_{n+1} = x''^P_{n+1} + 2\Delta x\, I_2/H^2_{n+1}, \tag{13}$$

where Δy and Δx are the differences of the predicted and corrected values, respectively. I_1 and I_2 are constant values, which depend on the integral step size as:

$$I_1 = \frac{2H_{n+1} + H_n}{H_{n+1} + H_n}, \tag{14}$$

$$I_2 = \frac{H_{n+1}}{H_{n+1} + H_n}. \tag{15}$$

To solve the differential equation represented in (1), Gear's method defines a new function U based on (1) and (3) as a replacement of the function f presented in (1). U_{n+1} is extracted from the main nonlinear differential equation presented in (1) and the corrected value of the first derivative (y'_{n+1}) presented in (3).

$$\begin{aligned} U_{n+1} &= y'_{n+1} - f(y_{n+1},\, x_{n+1},\, t_{n+1}) = 0 \\ U_{n+1} &= H_{n+1} y'^P_{n+1} + I_1\, \Delta y - H_{n+1}\, f\left(y^P_{n+1} + \Delta y,\, x^P_{n+1}\right. \\ &\quad \left. +\ \Delta x,\, t + H_{n+1}\right) = 0. \end{aligned} \tag{16}$$

U is a newly defined differential equation presented in (16), and g is the algebraic equation presented in (1). The new DAE is converted to a system of Ordinary Differential Equation (ODE) by differentiating it with respect to the variables as:

$$\begin{aligned} \Delta U &= U_{n+1} - U_n = U_{n+1} \\ &= \frac{\partial U}{\partial y}\Delta y + \frac{\partial U}{\partial x}\Delta x \\ &= I_1 - H\,\frac{\partial f}{\partial y} - H\,\frac{\partial f}{\partial x}, \end{aligned} \tag{17}$$

$$\Delta g = g_{n+1} - g_n = g_{n+1} = \frac{\partial g}{\partial y}\Delta y + \frac{\partial g}{\partial x}\Delta x, \tag{18}$$

and they are represented in a matrix form as:

$$\begin{bmatrix} U_{n+1} \\ g_{n+1} \end{bmatrix} = \begin{bmatrix} I_1 - H\,\frac{\partial f}{\partial y} & -H\,\frac{\partial f}{\partial x} \\ \frac{\partial g}{\partial y} & \frac{\partial g}{\partial x} \end{bmatrix} \begin{bmatrix} \Delta y \\ \Delta x \end{bmatrix}. \tag{19}$$

The only unknown variables in (19) are Δy and Δx, which are computed by finding the roots of the system ($U_{n+1} = 0, g_{n+1} = 0$). Newton-Raphson is a well-known method for finding the roots of coupled nonlinear equations. Changes to variables (Δx and Δy) to approximate the next step solution are calculated by solving (19). However, in the updating stage of Gear's method, the integral step size is adjusted by an internal loop based on the approximation error. The flowchart of Gear's method is shown in Figure 2. According to the flowchart, the accuracy of the approximation is checked by the Truncation Error (TE) defined by (20):

$$TE = |z(t_{n+1}) - z_{n+1}| = 2K_2\, I_2\, ||\Delta z||, \tag{20}$$

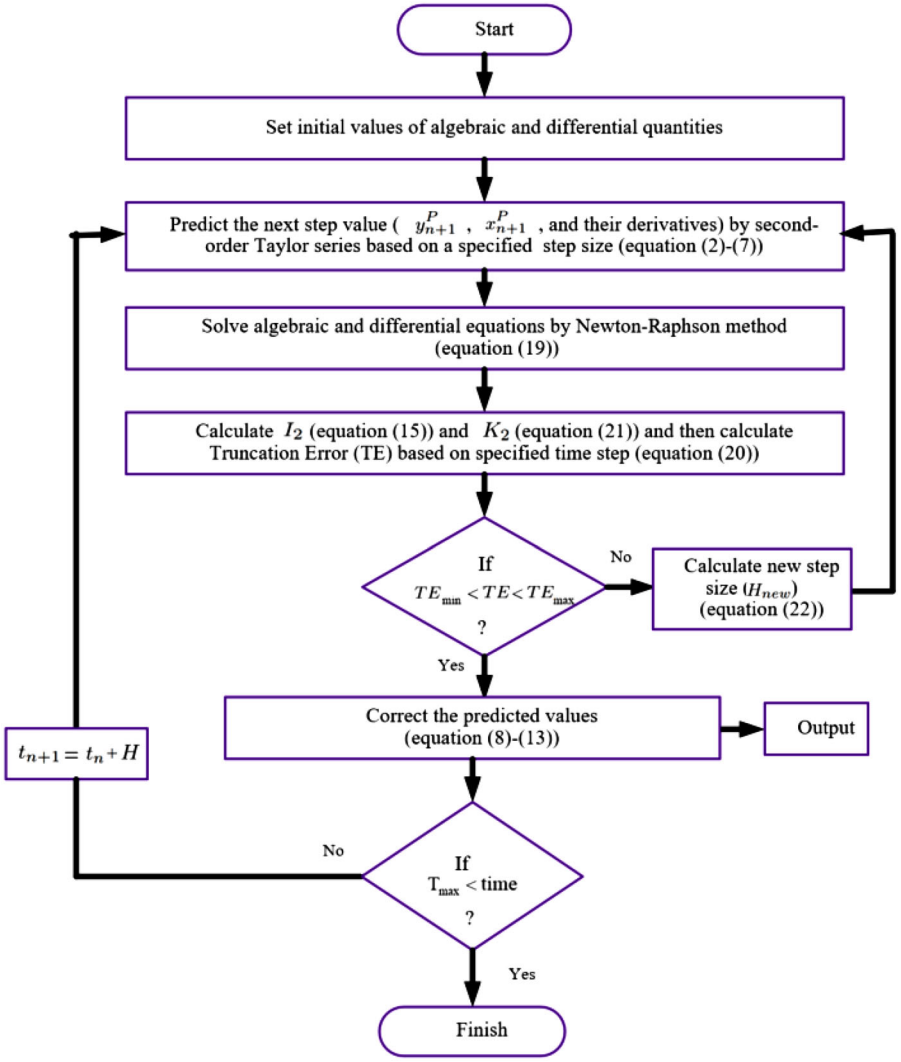

FIGURE 2 Flowchart of Gear's method

where $\mathcal{Z} = [y, x]$ is a global variable including both differential and algebraic variables and K_2 is:

$$K_2 = \frac{(H_{n+1} + H_n)^2}{6H_{n+1}(2H_{n+1} + H_n)}. \tag{21}$$

Based on the calculated Truncation Error (TE), the integral step size of the algorithm is adapted as [19]:

$$H_{new} = K_{sc} \sqrt{\frac{TE_{ds}}{2K_2\, I_2\, ||\Delta \mathcal{Z}||}}\, H_{old}, \tag{22}$$

where TE_{ds} is the desired accuracy. K_{sc} is a scaling factor smaller than one when decreasing the step size and is bigger than one when increasing the step size. The value K_{sc} is changed in each iteration to increase the numerical stability of the internal loop of the step size adaption in Gear's method.

3 | STATIC AND DYNAMIC EIGENVALUES IN UNIFIED STABILITY ANALYSIS

In addition to the numerical properties (accuracy and efficiency) of Gear's method, it can extract more information from the system, which can be utilized to analyze the system further and enrich our perception of its dynamic behavior. According to section 2, the linearization procedure inside Gear's method calculates the partial derivatives of differential and algebraic functions with respect to the variables. The partial derivatives form the state matrix (A) during both steady-state and dynamic conditions. The extracted A-matrix during steady-state will result in a static eigenvalue calculation according to the LTI system theory. However, transient conditions will result in a time-varying A-matrix that can be used to calculate dynamic eigenvalues and eigenvectors by LTV system theory [20]. Evaluating both concepts (static and dynamic eigenvalue) within the same framework is proposed in this paper to unify the

stability study of a power system. Differentiation of the algebraic equation presented in (1) gives:

$$0 = \frac{\partial g}{\partial y} y' + \frac{\partial g}{\partial x} x'. \tag{23}$$

Therefore, (23) yields the derivative of the algebraic variable as:

$$x' = -\left(\frac{\partial g}{\partial x}\right)^{-1} \frac{\partial g}{\partial y} f(y, x, t). \tag{24}$$

On the other hand, differentiation of the differential equation presented in (1) gives:

$$y'' = \frac{\partial f}{\partial y} y' + \frac{\partial f}{\partial x} x'. \tag{25}$$

After substitution of (24) for x', equation (25) yields:

$$y'' = \left(\frac{\partial f}{\partial y} - \left(\frac{\partial f}{\partial x}\left(\frac{\partial g}{\partial x}\right)^{-1} \frac{\partial g}{\partial y}\right)\right) y'. \tag{26}$$

Equation (26) is the linearized form of the nonlinear DAE presented in (1) and can be updated continuously during the simulation. Thus, the linearized representation implies [18]:

$$A = \frac{\partial f}{\partial y} - \left(\frac{\partial f}{\partial x}\left(\frac{\partial g}{\partial x}\right)^{-1} \frac{\partial g}{\partial y}\right), \tag{27}$$

where A is the state matrix of the system and is constant during steady-state conditions. Hence, static eigenvalues (λ) can be calculated from the extracted A-matrix for assessing the small-signal stability at any steady-state point during the simulation.

Access to the A-matrix of a power system during dynamic conditions enriches the large-signal stability analysis of a power system. During transient conditions, the extracted A-matrix of the stressed system will be time-varying, and at each step, we have:

$$Y'(t) = A(t)\, Y(t). \tag{28}$$

According to the LTV system theory, $\lambda_d(t)$ is a dynamic eigenvalue of the system if there is a dynamic eigenvector ($e_d(t)$) that satisfies the following equation:

$$A(t)\, e_d(t) = \lambda_d(t)\, e_d(t) + e'_d(t), \tag{29}$$

where $e'_d(t)$ is the derivative of the dynamic eigenvector. Contrary to the LTI system, the eigenvector derivative is also presented in the equation since it is not constant and changes over time. The correct dynamic eigenvector extracted for every dynamic eigenvalue forms a dynamic similarity matrix ($S_d(t) = [e_{d1}(t), e_{d2}(t), \ldots, e_{dn}(t)]$) by which the time-varying transient matrix (A(t)) can be transformed to the diagonal matrix as:

$$\Lambda = S^{-1}(t) A(t) S(t) - S^{-1}(t) S'(t), \tag{30}$$

where $S'_d(t)$ is derivative of the dynamic similarity matrix. Therefore, the dynamic eigenvalues will be on the transformed A-matrix's diagonal by applying the dynamic similarity transformation. To calculate the dynamic similarity transformation in the LTV system, we have to look for a function that satisfies equation (29). The control engineering literature states that a solution of the differential Riccati equation satisfies (29) [20–22].

Generally, for an A-matrix with dimension n, the n-order differential Riccati equation should be solved numerically [23]. For a second-order LTV system with state matrix ($A = [a_{11}(t), a_{12}(t); a_{21}(t), a_{22}(t)]$), the following equation (second order differential Riccati equation) should be solved [21]:

$$L'(t) = -a_{12} L^2(t) - (a_{11} - a_{22}) L(t) + a_{21}, \tag{31}$$

where $L(t)$ is the Riccati function. The Riccati function's solution and derivative are used in the dynamic eigenvalue and eigenvector calculation procedure. Accordingly, eigenvalues and eigenvectors during transient conditions will be calculated by equation (29). However, the stability of an LTV system cannot be evaluated just by monitoring the real-part of dynamic eigenvalues since the dynamic eigenvector also impacts the system's stability. Therefore, the impacts of both dynamic eigenvalues and eigenvectors are counted in the stability analysis by defining a Mode-Vector (MV) variable as [20]:

$$MV(t) = exp^{\int_{t_0}^{t} \lambda_d(\tau) d\tau}\, e_d(t). \tag{32}$$

The excursion of the MV shows the stability of each mode individually. According to the LTV system theory, a LTV system is stable if each MV norm is bounded. Being bounded or unbounded in this paper is determined by the Lyapunov Exponent (LE). LE is a stability certificate for the trajectory instead of the equilibrium point and provides information about the divergence and convergence of the system trajectory. The LE for excursion of the MV is calculated as:

$$LE = \lim_{t \to \infty} Re\left[\frac{1}{t} ln||e_d(t)|| + \frac{1}{t}\int_{t_0}^{t} \lambda_d(\tau) d\tau\right]. \tag{33}$$

In this index, the growth rate of the excursion of the MV is studied and compared with the exponential function. Meanwhile, for the real-time application, the time-window LE of the MV is calculated as [24, 25]:

$$LE(k\Delta t) = \frac{1}{Nk\Delta t} \times \sum_{m=1}^{N} log \frac{||MV((k+m)\Delta t) - MV((k+m-1)\Delta t)||}{||MV((m\Delta t)) - MV(((m-1)\Delta t))||}, \tag{34}$$

where samples from $m = 1$ to $m = N$ are in the window of analysis, $k\Delta t$ is the start of the window, and Δt is the step size. Since LE shows whether the excursion of a state is bounded or not, it is concluded that the LTV System is stable if the MV has a negative LE. Therefore, the stable and unstable modes during transient conditions are differentiated by the sign of the LE.

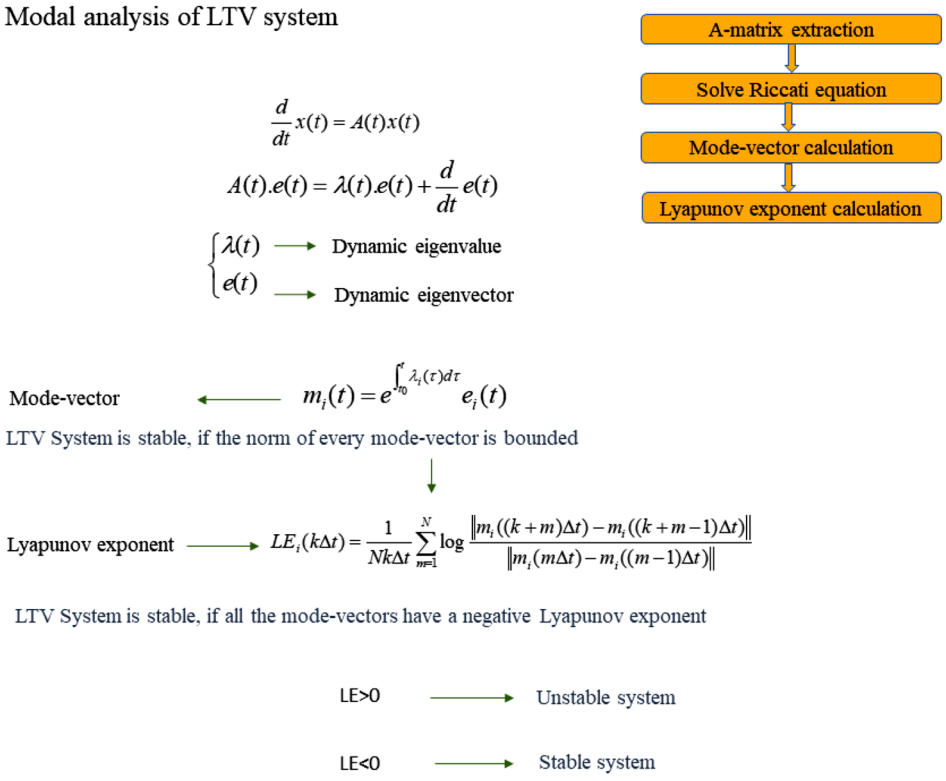

FIGURE 3 Summary of whole proposed method in this paper to analyze the stability of the system

The whole procedure of the power system stability analysis using the proposed method is shown in Figure 3. The LTV system analysis approach generalizes the LTI system analysis approach by involving both dynamic eigenvalues and dynamic eigenvectors in the stability analysis [20]. Dynamic eigenvalues and eigenvectors are calculated by solving a Riccati equation (as a general characteristic equation of a system). The *MV* is formed in the LTV system, and an excursion of *MV* shows the stability of the system. If *MV* is bounded, the LTV system is stable, and it is unstable if *MV* is unbounded. The *LE* is used to evaluate each *MV* of the state's excursion. If the *LE* of an *MV* is negative, the excursion is bounded, and it is unbounded when *LE* is positive. Therefore, a power system's stable or unstable behavior subjected to a severe disturbance is detected rapidly by the LTV system theory. [20].

The proposed method is conducted by four steps (Figure 3):

- A-matrix extraction
- Solve Riccati equation
- Mode-vector calculation
- Lyapunov exponent calculation

Finally, the sign of the *LE* shows the stability of the power system. The LE detects the stability of the system based on the trajectory of system states. If the LE is positive, the system is unstable and it is stable if the LE is negative.

4 | IMPLEMENTATION OF THE PROPOSED METHOD DURING LARGE-SIGNAL STABILITY ANALYSIS

Two issues are raised when dealing with large-signal disturbance analysis in the proposed method. The first is related to large-signal disturbance, and the second is related to saturation of limiters of control parts, which will be explained and solutions proposed in the following sections.

4.1 | Large-signal disturbances

The introduction of disturbances creates discontinuities in the integration process of Gear's method that a corrective approach should solve. According to the step size adaption technique, the solver tries to improve the estimate's accuracy by decreasing the step size at the instance of disturbance. However, due to the discontinuity, the Newton-Raphson's iteration loop cannot converge to the true value. In the proposed solver, a buffer matrix (matrix *Mat* presented in (35)) at the end of each step is stored temporarily in an external matrix and is updated at every step. When there is a disturbance (a fault occurs or a fault clears), a sub-function raises a flag and notifies the Newton-Raphson sub-function to replace the *Mat* matrix with the stored matrix from the previous step

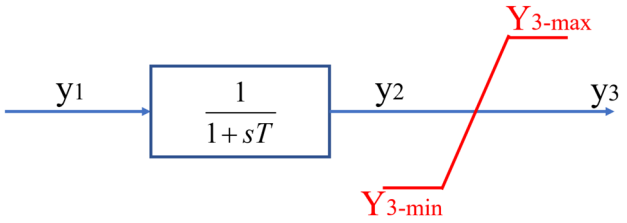

FIGURE 4 System with limiter

(Mat_{pre}) as:

$$Mat_{pre} = \begin{bmatrix} I_1 - H_{n-1}\dfrac{\partial f_{n-1}}{\partial y} & -H_{n-1}\dfrac{\partial f_{n-1}}{\partial x} \\ \dfrac{\partial g_{n-1}}{\partial y} & \dfrac{\partial g_{n-1}}{\partial x} \end{bmatrix}. \quad (35)$$

According to the proposed strategy, the Newton-Raphson method will be run with the recorded matrix (Mat_{pre}) only at the instance of the disturbance. Additionally, changing the reference of control of power electronic-based technologies creates some discontinuities in the integration process that is solved by replacing the previously stored matrix (Mat_{pre}) at the instance of change of reference.

4.2 | Limiters

Large-signal stability analysis is executed by simulating the whole power system. In large-signal stability analysis, limiters of control parts must be modeled when the system is exposed to severe disturbances. An extra algebraic equation is defined in the system to model a limiter in the solver. For example, consider the system with a limiter shown in Figure 4. The left part of the system is modeled by the following differential equation:

$$\frac{dy_2}{dt} = \frac{y_1 - y_2}{T}. \quad (36)$$

The model of the right part of the system in Figure 4 depends on whether the limiter is saturated or not. The following algebraic equation is valid in a normal condition (without saturation):

$$y_3 = y_2. \quad (37)$$

However, if y_3 is bigger than Y_{3-max} or smaller than Y_{3-min}, the last equation (equation (37)) is not valid. y_2 and y_3 will be disconnected and y_3 adapts a constant value without reflecting variation of y_2. The constant value of the algebraic variable (y_3) creates zero value (zero first- and second-derivatives) in the corresponding row and column of the matrix of the partial derivatives, so the matrix is singular. The saturation time step should be detected first to prevent the problem. This is done by continuously monitoring the output of the limiters. Whenever an output of a limiter passes the threshold (up or down limits), the corresponding row and column in the derivative matrix are detected and are removed from the matrix. In this way, the dimension of the corresponding matrices is decreased by one for every saturated limiter in both the prediction and the correction stages. By changing the dimension of the derivative matrix (Mat) in a saturation condition, the stored matrix (Mat_{pre}) should also be reproduced by a new dimension so that it can be used in the solver when it is necessary (instant of a disturbance).

5 | SIMULATION RESULTS

Three cases are studied in this section. First, a synthesised system to evaluate the performance of Gear's method is explored. Second, a single machine to an infinite bus (SMIB) is analyzed from small- and large-signal stability viewpoints. Finally, the performance of unified stability analysis is evaluated for a multi-machine power system with HVDC.

5.1 | Simulation results of performance of Gear's method applied to a synthesized system

A synthesized system (presented by (38)) is studied in this section to reveal the internal procedure of the implemented method.

$$\begin{aligned} \frac{d}{dt}y_1 &= y_2, \\ \frac{d}{dt}y_2 &= 1000\left(1 - y_1^2\right)y_2 - y_1, \end{aligned} \quad (38)$$

where y_1 and y_2 are two differential variables with initial conditions: $y_1(0) = 2$ and $y_2(0) = 0$. Gear's method is applied to (38) to evaluate the movements of the state variables throughout the time. Variation of y_1, step size, and Truncation Error (TE) are shown in Figure 5. It reveals that the solution y_1 has rapid changes around time = 800 s and time = 1600 s. The method identifies these conditions by monitoring the TE and comparing it with a threshold range. According to Figure 5, the step size decreases considerably when the rate of change is high (time = 800 s and time = 1600 s), while the step size increases when the rate of change is lower. Using adaptive time steps while keeping the numerical integration accurate even under rapid changes are two properties of Gear's method, making it a promising solver for AC/DC power systems with different time constants.

5.2 | Single machine to infinite bus (SMIB)

In this section, performance of Gear's method is evaluated by simulating a SMIB during steady state and dynamic conditions. This system is presented in [26], with small-signal analysis done in chapter 12 and large-signal analysis in chapter 13, respectively. The generator (G1) shown in Figure 6 produces an apparent power $S_{Bus1} = 0.9 + j0.436$ (in per-unit) at Bus1 with voltage $V_{Bus1} = 1.0\angle 28.34^0$ during steady state. The generator is presented by a second-order model with an internal voltage

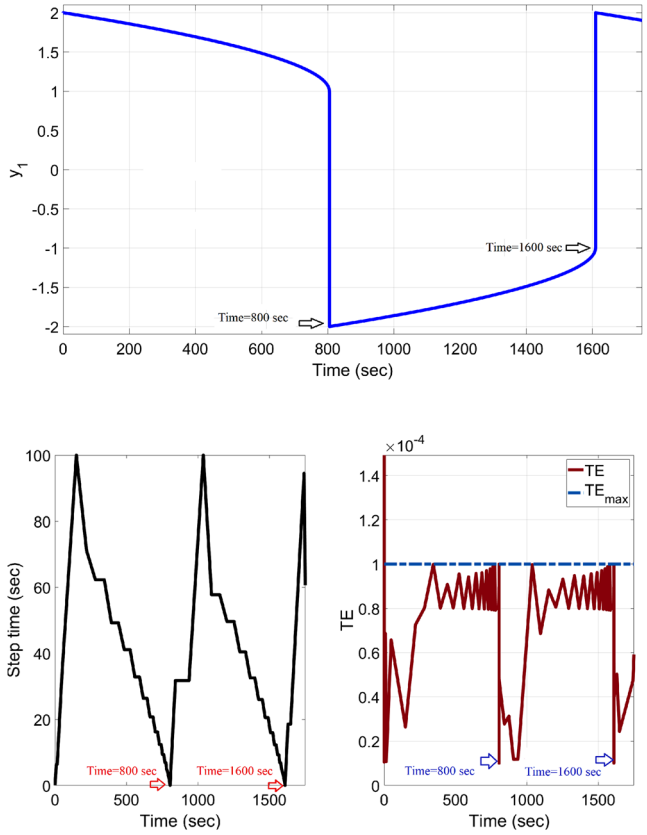

FIGURE 5 Simulation results of synthesized system

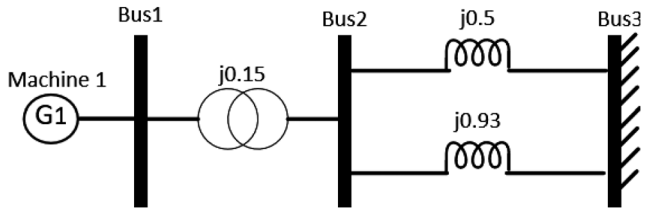

FIGURE 6 Single machine to infinite bus (SMIB)

($E'\angle\delta$) behind a transient reactance $X'_d = 0.3$p.u., inertia constant $H_{int} = 3.5$ s and damping factor $K_D = 25$. It is connected to an infinite bus ($V_{Bus3} = 0.90081\angle 0$) through the network, which is shown in Figure 6. A classical generator model is initially used in this section to facilitate the explanation of the method and illustrate its key properties. A higher order model of the generator will be used in the next section.

5.2.1 | Small-signal stability analysis

The method simulates the SMIB numerically based on the predictor-corrector and adaptive step size strategies to show an efficient and accurate performance. The method can extract the linearized equations continuously and therefore, the state matrix in each integration step is available. The state matrix (A), extracted by Gear's method, has for the steady state ($0 < t <$ 2 s) eigenvalues (λ) :

$$A = \begin{bmatrix} -3.5714 & -0.1439 \\ 376.9911 & 0 \end{bmatrix}, \lambda = -1.7857 \pm 7.1468i. \quad (39)$$

The small-signal analysis shows that there are two complex eigenvalues with negative real-part associated with the dynamics of the rotor. Therefore, it is anticipated that the system will show a damped oscillatory time response when subjected to a non-severe disturbance. The same results are obtained in chapter 12 in [26].

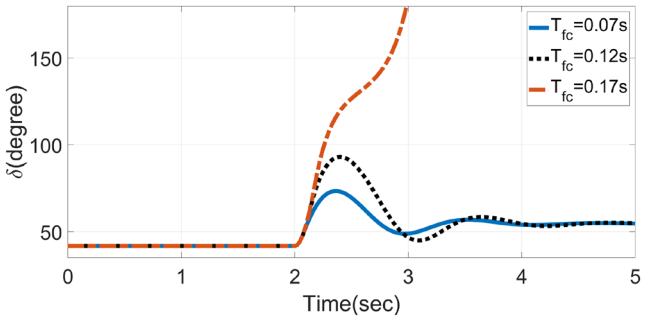

FIGURE 7 Rotor angle responses for different values of T_{FC} in SMIB

5.2.2 | Large-signal stability analysis

As the primary duty of a numerical method, transient stability analysis of a SMIB is done using Gear's method in this part. Different fault conditions are applied to the simulated power system for evaluating the large-signal stability via a numerical integration. The power system is simulated for three different fault clearing times ($T_{FC} = 0.07, 0.12, 0.17$ s). A three-phase fault occurred at Bus 2 at time = 2 s and is cleared by removing the transmission line with impedance $j0.93$, and the results are shown in Figure 7. The results indicate that the system is stable with $T_{FC} = 0.07$ s and $T_{FC} = 0.12$ s, and is unstable with $T_{FC} = 0.17$ s.

5.2.3 | Detection of instability

Dynamic eigenvalues and eigenvectors are proposed in this paper to detect the instability and stop the numerical simulation. The differentiation between stable and unstable trajectories is done by solving a Riccati equation. The performance of the proposed method in the SMIB system is shown in this section. A three-phase fault occurred in the power system (shown in Figure 6) at Bus 2 at time = 2 s and is cleared by removing the transmission line with impedance $j0.93$. Two cases will be evaluated here: stable and unstable conditions. Firstly, the fault duration is selected to 0.07, and the simulation results are shown in Figure 8. According to the proposed method, the excursion of the MV (dynamic eigenvalues and eigenvector) are calculated (Figure 8), which indicates that MV is bounded. The LEs of the MV are also presented in Figure 8, which has negative

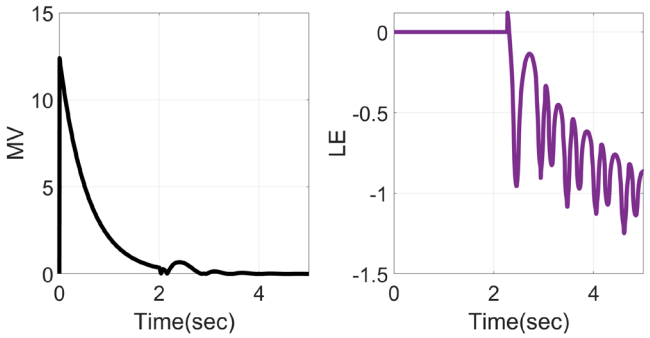

FIGURE 8 Stable condition, mode-vector (MV) and Lyapunov exponent (LE)

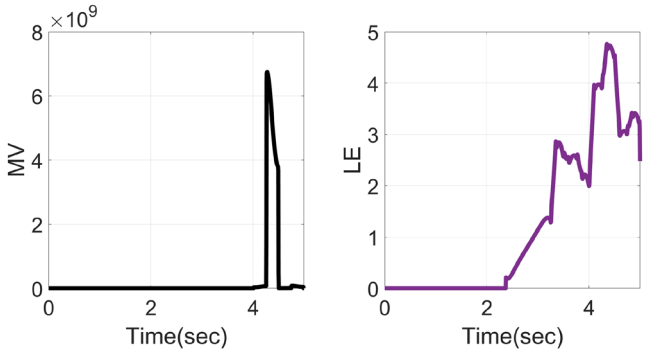

FIGURE 9 Unstable condition, mode-vector (MV) and Lyapunov exponent (LE)

values after removing the fault, and accordingly, the system is stable. A simulation is run when the fault lasts 0.17 s, and the results are shown in Figure 9. According to Figure 9, the system is unstable since the calculated *LE*s are positive after removing the fault. Therefore, it is possible to detect the unstable condition by applying the proposed method, allowing us to stop the simulation earlier.

5.2.4 | Unified stability analysis

The proposed method allows for unified stability analysis, which combines the small- and large-signal analysis into one procedure. It is illustrated in Figure 10, which shows the performance of the SMIB during successive events. In the proposed framework, it is possible to switch from small- signal to large-signal and from large-signal to small-signal analysis, as shown in Figure 10. Six different successive conditions are considered (three steady-state and three transient conditions) in this section. From time=0 s to time=2 s, the system is in the steady-state condition (steady-state 1). The method evaluates the system's small-signal stability by extracting the A-matrix and then calculating the static eigenvalues (static λ). At time = 2 s, a three-phase fault occurs at Bus 2 and is removed at 0.07 s by disconnecting the line with impedance $j0.93$. The severe fault forces the power system into a transient condition (Transient 1) during which the classical eigenvalue is not applicable. However,

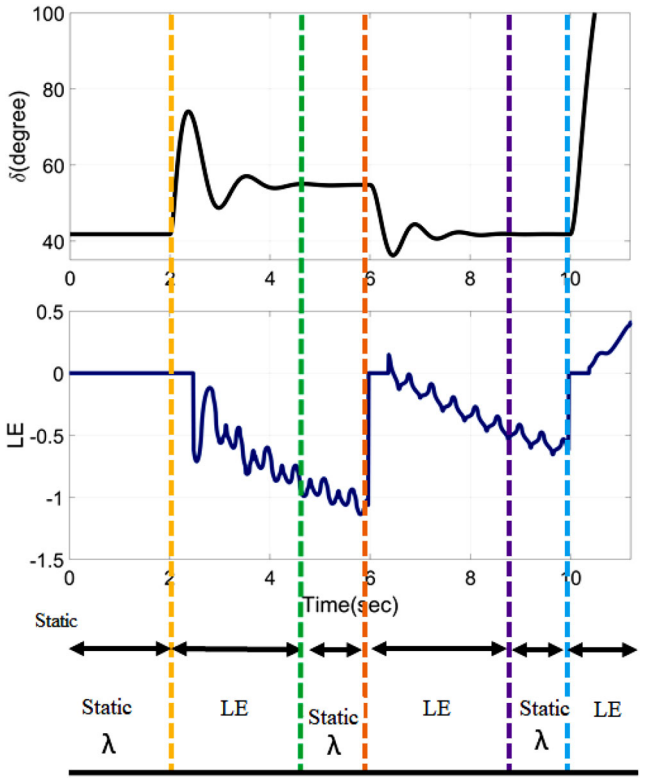

FIGURE 10 Unified stability analysis in SMIB with six different conditions

according to the proposed method, the negative sign of *LE* shows that the system is stable. When the system's trajectory settles to a new steady-state condition (steady-state 2), the small-signal analysis is run again, and the static eigenvalues move due to a change of structure of the power system (removing the line). At time = 6 s, another severe disturbance occurs by re-closing the line (impedance $j0.93$), and the system goes into a transient condition (Transient 2). Again the Riccati equation is calculated based on the extracted A-matrix, and the results show that *LE* is negative and therefore, the system is stable under this transient condition. The next condition (steady-state 3) is when the oscillation is damped, and the method extracts the A-matrix and detects the stable condition by negative static eigenvalue. The third transient event is a step increase in the generator's mechanical power at time = 0 s from 0.9 to 1.4 p.u. The calculated *LE* is positive, which shows that the system is unstable. The explained procedure demonstrates that the small- and large-signal analysis can be done in sequence with just one procedure. Therefore, the proposed method provides a unified stability analysis in addition to an efficient and numerically accurate integration operation.

5.3 | Multi-machine power system with HVDC

Consider the WSCC power system shown in Figure 11. A three-generator power system (Figure 11a) is simulated numerically in

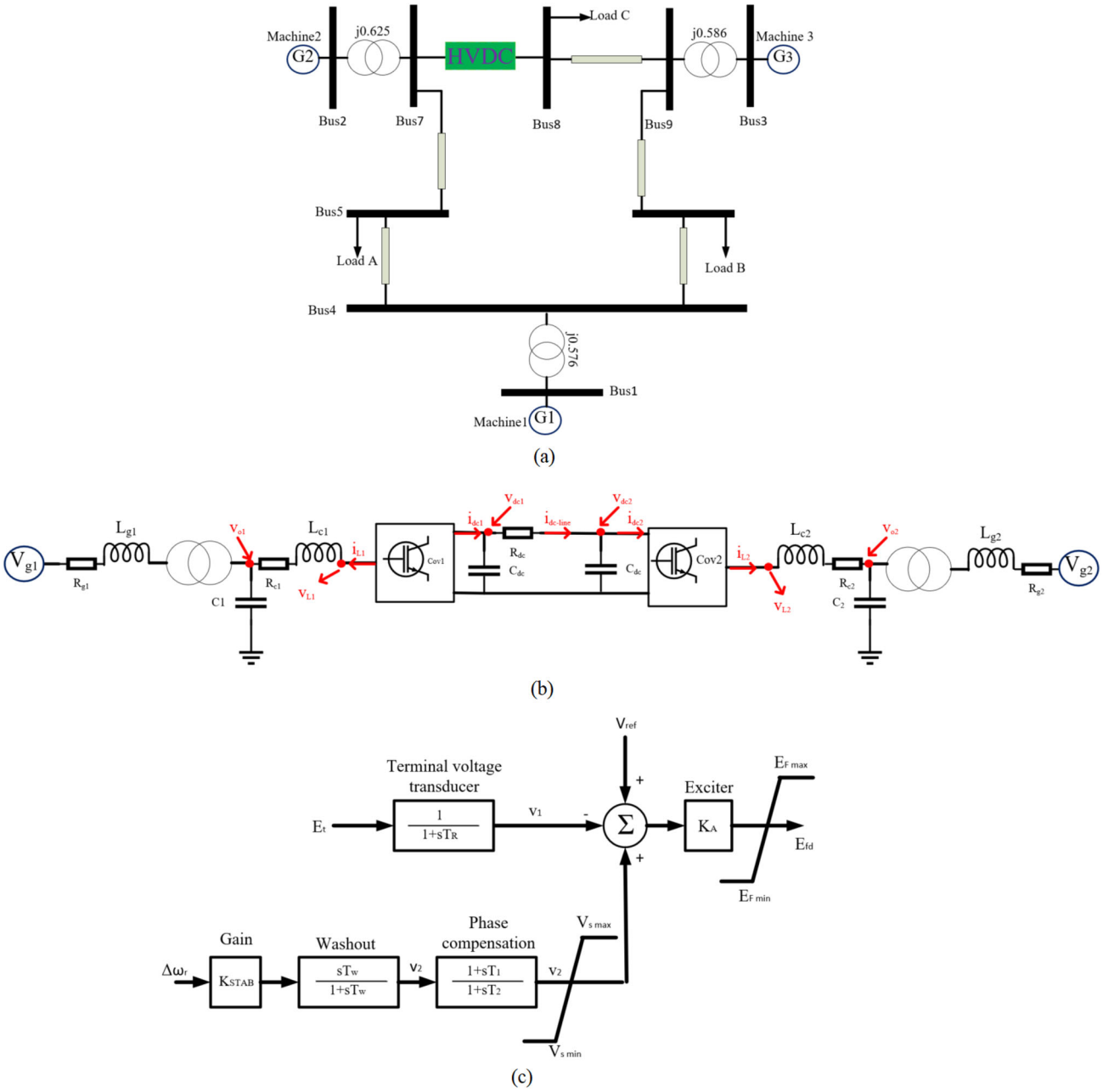

FIGURE 11 Three-generator and nine-bus power system (WSCC), HVDC link between Bus 7 and 8, AVR-PSS

this section to evaluate the performance of Gear's method in a multi-machine AC/DC power system (details of HVDC link is shown in Figure 11b). The system represents an approximation of the Western System Coordinating Council (WSCC), and its data are presented in [27]. The multi-machine power system is modeled by the current injection method presented in [28, 29]. The AC transmission lines and the loads are also considered using the phasor models in the admittance matrix. Since there is no infinite bus in the system, the rotor angle of machine-1 (G1) is considered as reference, and generator's angles are calculated with respect to the G1. In steady-state condition, G1 as a slack generator produces an apparent power $S_{Bus1} = 0.716 + j0.270$, G2 produces $S_{Bus2} = 1.63 + j0.665$, and G3 produces $S_{Bus3} = 0.85 - j0.108$.

5.3.1 | AVR and PSS

A generator is equipped with an automatic voltage regulator (AVR) and a power system stabilizer (PSS) to enhance the oscillation damping in dynamic conditions. Detailed presentation of the AVR and the PSS systems are shown in Figure 11c [26]. In addition to the two equations corresponding to the mechanical part of the generator, four complementary equations are

added to the DAE's system to represent the generator+AVR+PSS.

E_{fd} is the exciter output voltage, K_A is the gain of exciter, T_r is the delay time of the controller of the AVR, E_{fmin} and E_{fmax} are thresholds of limiting the output from the PSS, T_w is coefficient of washout filter, K_{stab} is the gain of PSS, T_1 and T_2 are coefficients of the controller of PSS, and v_{smin} and v_{smax} are the thresholds of limiter in the output of the PSS.

In addition to the swing equation of the SMIB, four complementary equations are added to the system of the DAE to simulate the power system of this section. The four differential equations are:

$$\frac{d}{dt}\psi_{fd} = \frac{\omega_0 R_{fd}}{L_{ads}} E_{fd} - \omega_0 R_{fd} i_{fd}, \tag{40}$$

$$\frac{d}{dt}v_1 = \frac{1}{T_r}(E_t - v_1), \tag{41}$$

$$\frac{d}{dt}v_2 = \underbrace{\frac{K_{stab}}{2H_{int}}(T_m - T_e - K_D\Delta\omega_r)}_{\text{SE}} - \frac{1}{T_w}v_2, \tag{42}$$

$$\frac{d}{dt}v_s = \frac{1}{T_2}(v_2 - v_s + T_1(SE) - \frac{1}{T_w}v_2), \tag{43}$$

where the excitation system is modeled by (40), equation (41) represents the AVR, and equations (42) and (43) are related to the PSS. $R_{fd} = 6 \times 10^{-4}$ and $L_{ads} = 1.3726$ are resistance and inductance of the field circuit, E_{fd} is the exciter output voltage, i_{fd} is the field current, $K_A = 200$ is the gain of exciter, $T_r = 0.015$ is the coefficient of controller of AVR, and $E_{fmin} = -6.4$ and $E_{fmax} = +7$ are the thresholds of the limiter's output from the PSS. $T_w = 1.4$ is the coefficient of washout filter, $K_{stab} = 9.5$ is the gain of PSS, and $T_1 = 0.1540$ and $T_2 = 0.033$ are the coefficients of controller of PSS, while $v_{smin} = -0.1$ and $v_{smax} = +0.1$ are the thresholds of limiter in output of the PSS.

5.3.2 | HVDC link

The HVDC link between Bus 7 and Bus 8 consists of electrical (AC and DC) and control parts, in which the dynamic models presented in [30] are used in this paper. The electrical part of the HVDC is shown in Figure 11b. The rectifier-side (Conv1) of HVDC controls the DC voltage (v_{dc1}) and reactive power (Q_1), and inverter-side (Conv2) controls the active (P_2) and the reactive power (Q_2) at the associated buses (Bus7 and Bus8). In steady-state condition, reference values of the HVDC are: $v_{dc1} = 1$, $Q_{ref1} = -0.0704$, $P_{ref2} = 0.7590$, and $Q_{ref2} = 0.0302$ (all are per unit).

The stability of the system with a HVDC link is also included in this paper. In this paper, the converter model includes both fast and slower transients. Thus, both the electrical and control parts of converters in the HVDC link are represented by dynamic models. Consider a full HVDC link in Figure 11b. According to Figure 11b, the right-side converter is a PQ converter used to control active and reactive power at PCC in an HVDC link. Different internal parts of a PQ converter (electrical and control parts) will be explained in the following subsections.

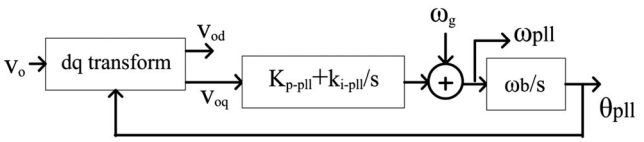

FIGURE 12 Phase locked loop

VSC (voltage source converter) of the converter is modeled by the following equations:

$$\frac{d}{dt}i_{Ld} = \frac{\omega_g\omega_b}{L_c}v_{Ld} - \frac{\omega_g\omega_b}{L_c}v_{od} - \frac{\omega_g\omega_b R_c}{L_c}i_{Ld} + \omega_g\omega_b i_{Lq},$$

$$\frac{d}{dt}i_{Lq} = \frac{\omega_g\omega_b}{L_c}v_{Lq} - \frac{\omega_g\omega_b}{L_c}v_{oq} - \frac{\omega_g\omega_b R_c}{L_c}i_{Lq} - \omega_g\omega_b i_{Ld}, \tag{44}$$

where parameters and variables presented in (44) are in the per-unit system and are shown in Figure 11b. All parameters and variables of rectifier-side (PQ converter) are labeled by '1', and inverter-side (QV converter) are marked by '2' in Figure 11b. ω_g and ω_b are grid and base angular frequencies, respectively. Additionally, the shunt branch in the PQ converter (Figure 11b) is modeled as:

$$\frac{d}{dt}v_{od} = \omega_g\omega_b C_f i_{Ld} - \omega_g\omega_b C_f i_{od} + \omega_g\omega_b v_{oq},$$

$$\frac{d}{dt}v_{oq} = \omega_g\omega_b C_f i_{Lq} - \omega_g\omega_b C_f i_{oq} - \omega_g\omega_b v_{od}. \tag{45}$$

Moreover, there are three control loops in the control part of a PQ converter: phase lock loop (PLL), outer and inner loops to achieve the control goals.

5.3.2.A. Phase lock loop (PLL)

To synchronize the output of VSC with the voltage at PCC, a Phase Locked Loop (PLL) is used (Figure 8) with the following dynamic model:

$$\frac{d}{dt}\epsilon_{pll} = v_{oq},$$

$$\frac{d}{dt}\delta\theta_{pll} = \omega_b(k_{p-pll}\, v_{oq} + k_{i-pll}\, \epsilon_{pll}), \tag{46}$$

where variables presented in (46) are shown in Figure 12. The phase-locked loop (PLL) block is a feedback control system that automatically adjusts a locally generated signal phase to match the phase of an input signal.

5.3.2.B. Outer controller

The outer loop controller (Figure 13) used in a PQ converter to control the active and reactive power at Point of Common

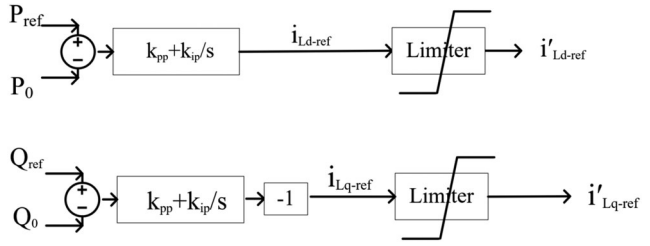

FIGURE 13 Outer controller of a PQ converter

Coupling (PCC) as:

$$\begin{aligned}
\frac{d}{dt}\gamma_P &= P_{ref} - P_o,\\
\frac{d}{dt}\gamma_Q &= Q_{ref} - Q_o,\\
i_{Ld-ref} &= +1(k_{pp}(P_{ref} - P_o) + k_{ip}\gamma_P),\\
i_{Lq-ref} &= -1(k_{pp}(Q_{ref} - Q_o) + k_{ip}\gamma_Q),\\
P_o &= v_{od}i_{od} + v_{oq}i_{oq},\\
Q_o &= v_{oq}i_{od} - v_{od}i_{oq},
\end{aligned} \tag{47}$$

where γ_P and γ_Q are the integrator states of the PI controllers, while other parameters and variables presented in (47) are shown in Figure 13. Additionally, two limiters are located at the end of PI controllers that are modeled with two algebraic equations as:

$$\begin{aligned}
0 &= i'_{Ld-ref} - (k_{pp}(P_{ref} - P_o) + k_{ip}\gamma_P),\\
0 &= i'_{Lq-ref} - (k_{pp}(Q_{ref} - Q_o) + k_{ip}\gamma_Q),
\end{aligned} \tag{48}$$

where these two equations keep the output of PI controller inside two limit values (up and down limits).

5.3.2.C. Inner controller

The output signals from the outer controllers (i'_{Ld-ref} and i'_{Lq-ref}) are sent to the inner loop current controller which provide the references of voltage (v_{Ld-ref} and v_{Lq-ref}). The inner loop (shown in Figure 14) is modelled dynamically by two equations as:

$$\begin{aligned}
\frac{d}{dt}\gamma_{id} &= i_{Ld-ref} - i_{Ld}\\
\frac{d}{dt}\gamma_{iq} &= i_{Lq-ref} - i_{Lq}\\
v_{Ld-ref} &= k_{pc}(i'_{Ld-ref} - i_{Ld}) + k_{ic}\gamma_{id} + v_{od} - \omega_{pll}L_c i_{Lq}\\
v_{Lq-ref} &= k_{pc}(i'_{Lq-ref} - i_{Lq}) + k_{ic}\gamma_{iq} + v_{oq} + \omega_{pll}L_c i_{Ld},
\end{aligned} \tag{49}$$

where γ_{id} and γ_{iq} are the integrator states of the PI controllers. Other parameters and variables presented in (49) are shown in Figure 14.

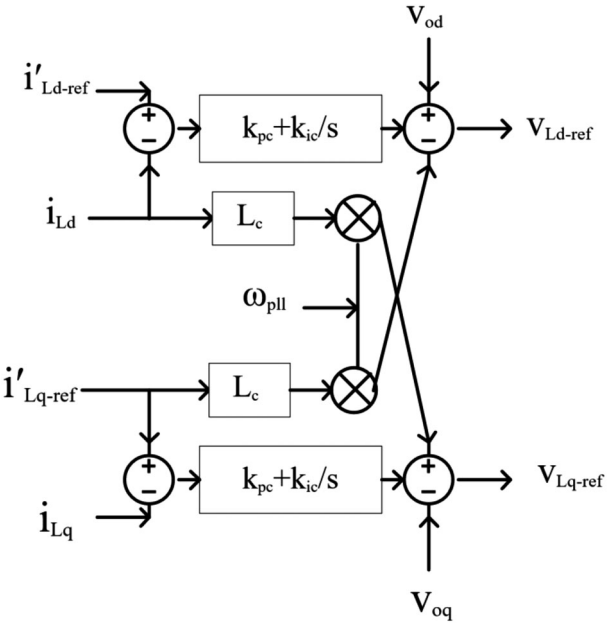

FIGURE 14 Inner controller of a PQ converter

Modeling the QV converter of a complete HVDC system is similar, but the difference is in the outer control. QV converter is used to control reactive power at PCC and DC voltage of DC link. Since the models of the VSC internal control, filters, and PLL of QV converter are the same as for the PQ converter, they will not be repeated here.

Since there are many state variables in the electrical and control parts of the AC/DC system, an automatic procedure is employed in this paper to obtain the appropriate initial condition for the start of the numerical simulation. Time is set to zero and the results of the power flow are sent to the initialization stage. In the initialization stage, the prediction stage and step size adaption technique of the method are bypassed, and only the correction stage is used. Therefore, the initial values of all states are calculated by iterations of the Newton-Raphson method and then they are taken into account to generate an accurate starting point of the simulation.

According to the calculated initial values, the method simulates the whole AC/DC system numerically and extracts the A-matrix of the power system during simulation, by which small-signal stability analysis is conducted during the steady state condition. Gear's method is applied to the DAE system (multi-machine AC/DC system), and the extracted eigenvalues, state (participation factor), and associated parts (EL(AC)= AC electrical parts, EL(DC)= DC electrical parts, GN=Generators , CONT= Control parts, EXC= Excitation of generator, AVR and PSS) are tabulated in Table 1. γ_{id}, γ_{iq}, γ_P, γ_Q, and γ_{dc} are mathematical variables defined in the dynamic model of an HVDC interconnection [30], but the other variables presented in Table 1 are shown in Figure 11. Table 1 presents a wide range of time constants due to the different types of elements in the power system. It is worth noting that the presented results (small-signal analysis) in this section were usually extracted in the literature by running the individual simulation

TABLE 1 Eigenvalues of WSCC with HVDC

Number	Eigenvalue	State (PF)	Part
1,2	$10^4 \times (-0.1018 \pm 1.1060i)$	io_2 (0.3075)	EL(AC)
3,4	$10^4 \times (-0.0266 \pm 1.0015i)$	io_1 (0.2792)	EL(AC)
5,6	$10^4 \times (-0.0164 \pm 0.7057i)$	vo_1 (0.2785)	EL(AC)
7,8	$10^4 \times (-0.0556 \pm 0.6239i)$	vo_2 (0.3092)	EL(AC)
9	$10^4 \times (-0.4254)$	v_{dc1} (0.5015)	EL(DC)
10	$10^4 \times (-0.0310)$	i_{Lq2} (0.7363)	EL(AC)
11	$10^4 \times (-0.0276)$	i_{Lq1} (1.1757)	EL(AC)
12	$10^4 \times (-0.0273)$	i_{Ld2} (0.8033)	EL(AC)
13	$10^4 \times (-0.0228)$	$\delta\theta_{pll1}$ (1.0324)	CONT
14	$10^4 \times (-0.0218)$	$\delta\theta_{pll2}$ (1.0419)	CONT
15	$10^4 \times (-0.0214)$	i_{Ld1} (1.2467)	EL(AC)
16,17	$10^4 \times (-0.0002 \pm 0.0018i)$	γ_{Q2} (0.6403)	CONT
18	$10^4 \times (-0.00254)$	γ_{id2} (0.8115)	CONT
19	$10^4 \times (-0.00250)$	γ_{iq1} (0.8464)	CONT
20	$10^4 \times (-0.0022)$	γ_{id1} (1.1184)	CONT
21,22	$-1.8595 \pm 13.1914i$	δ_3 (0.4549)	GN3
23,24	$-0.8639 \pm 8.6159i$	δ_2 (0.3904)	GN2
25	-14.4503	γ_{P2} (0.6618)	CONT
26	-14.0136	γ_{Q1} (0.7006)	CONT
27,28	$-2.0120 \pm 2.9074i$	γ_{dc1} (0.5901)	CONT
29	-2.3562	ϵ_{pll1} (1.4907)	CONT
30	-2.3583	ϵ_{pll2} (1.4932)	CONT
31	-50.6599	ψ_{fd} (0.402)	EXC
32	-0.7392	v_1 (1.01)	AVR
32,33	$-21.97 \pm 15.31i$	v_3 (0.82)	PSS

based on the linear models, but this method extracts them when the non-linear numerical integration is running.

Gear's method also allows for analysing the dynamic performance of a power system under severe disturbances (large-signal stability analysis). It is done by simulating the whole system with different fault clearing times. However, contrary to the small-signal analysis, limiters of the control parts of HVDC, AVR, and PSS must be modeled when the system is exposed to severe disturbances. Limiters introduce upper and lower limits of the variables. Under transient conditions, the control variable reaches the limit values, and there will be a constant value with zero first- and second-order derivatives. The method is also applied to the DAE system corresponding to the WSCC system with HVDC, and it is evaluated from a large-signal stability analysis viewpoint. A three-phase fault occurs at Bus 7 at time = 1 s and is cleared by different clearing times ($T_{fc} = 0.10, 0.26, 0.27$). Variation of the rotor angle responses of the generators (G2 and G3 with respected to G1) subjected to the three-phase fault are shown in Figure 15 ($T_{fc} = 0.10$ (Figure 11a), 0.26 (Figure 11b),0.27 (Figure 11c)). According to Figure 15, the system is stable when the fault lasts between 0.10 s and 0.26 s. However, if fault lasts 0.27 s, the system will lose its synchronization. Therefore, the critical clearing time is 0.26s.

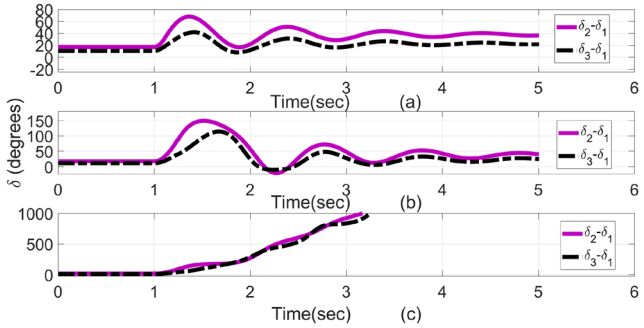

FIGURE 15 Rotor angle responses and step size variation for stable condition in WSCC-HVDC

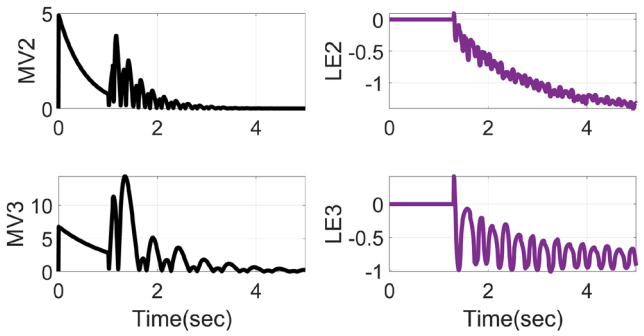

FIGURE 16 Stable condition, mode-vector (MV) and Lyapunov exponent (LE)

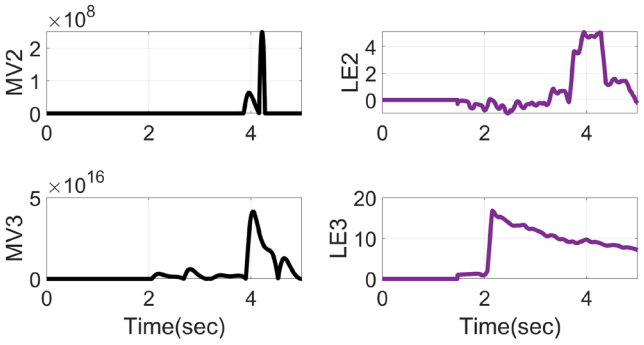

FIGURE 17 Unstable condition, mode-vector (MV) and Lyapunov exponent (LE)

The proposed method based on dynamic eigenvalues and the *LE* is also applied in this section by solving the matrix Riccati equation. The power system shown in Figure 11 is evaluated under two fault conditions: A three-phase fault occurs at Bus 7 at time = 1 s and is cleared by two clearing times $T_{fc} = 0.1$ and $T_{fc} = 0.27$. The results (MVs and LEs) of two cases are shown in Figures 16 and 17. Figure 16 depicts a stable condition in which *MV*s of G_2 and G_3 are bounded. Therefore, the *LE* of both mode vectors are negative after removing the fault at time = 1.1 s. On the other hand, Figure 17 shows a power system with an unstable excursion of states. The *MV*s of generators are unbounded after a long lasting fault ($T_{fc} = 0.17$), which is determined quantitatively by a positive sign of the *LE*s.

Therefore, the byproduct of Gear's method (A-matrix) can shed more light on the transient performance of a power system with LTV system theory.

6 | CONCLUSION

A framework for unified analysis of large-signal and small-signal stability is proposed in this paper on basis of Gear's method for numerical simulation. The use of Gear's method allows for time-domain simulation of DAE systems by self-adaptive step size while extracting the A-matrix of the linearized system model at any point during the simulation. Thus, this work presents a step towards a potential alternative to the classical approaches for power system stability analysis by conducting small- and large-signal analyses separately by different tools. Instead, the small-signal dynamics can be studied by applying established techniques for LTI system analysis to the A-matrix obtained at any steady-state operating point during the simulation. Furthermore, the calculation of the A-matrix during numerical simulation of large-signal transients also enables analysis of the studied power system configuration as a LTV system where dynamic eigenvalues and dynamic eigenvectors can be evaluated. The presented approach evaluates the excursion of the MV variable, which consists of both dynamic eigenvalues and dynamic eigenvectors. Then the LE method is applied to each MV to evaluate if it is bounded or not. If all calculated LEs of the system are negative, all MVs will be bounded, implying that the system is stable. On the other hand, an unstable mode is detected by a positive LE value during time-varying conditions. Therefore, the proposed framework can utilize the properties of Gear's method to monitor and then distinguish the power system stability conditions during both steady-state conditions and large-signal transients. To validate the contributions of the method in stability analysis, three examples of systems were evaluated as test cases and the results show that Gear's method can be used as an efficient and unified solver for comprehensive stability analysis of a power system. It should be noted that the proposed approach for analysis of static and dynamic eigenvalues during time-domain simulation also could be adapted to any other numerical method that can provide continuous access to the A-matrix of the system. However, Gear's method is utilized as a framework in this paper since it is conveniently configured for providing the required information while enabling self-adaptive time-step simulation of numerically stiff systems. Although explicit analysis of the A-matrix will increase the computational requirements for the time-domain simulation, it does not have to be conducted in each time step. Thus, further work could include development of criteria for identifying when the static or dynamic eigenvalues should be evaluated to ensure that critical information on the stability properties of the studied system is extracted while minimizing the computational requirements.

FUNDING INFORMATION

The author(s) received no specific funding for this work.

CONFLICT OF INTEREST

The authors have declared no conflict of interest.

ORCID

Jalal Khodaparast https://orcid.org/0000-0002-2874-7566

REFERENCES

1. Eladany, M.M., Eldesouky, A.A., Sallam, A.A.: Power system transient stability: An algorithm for assessment and enhancement based on catastrophe theory and facts devices. IEEE Access 6, 26424–26437 (2018)
2. Alsakati, A.A., Vaithilingam, C.A., Alnasseir, J., Jagadeeshwaran, A.: Simplex search method driven design for transient stability enhancement in wind energy integrated power system using multi-band pss4c. IEEE Access 9(1), 83913–83928 (2021)
3. Huang, L., Xin, H., Dörfler, F.: H-control of grid-connected converters: Design, objectives and decentralized stability certificates. IEEE Trans. Smart Grid 11(5), 3805–3816 (2020)
4. Cai, Y., Zhang, J., Yu, W.: A predictor-corrector method for power system variable step numerical simulation. IEEE Trans. Power Syst. 34(4), 3283–3285 (2019)
5. Serrano Jiménez, D., Unamuno, E., Gil-de Muro, A., Aragon, D.A., Ceballos, S., Barrena, J.A.: Stability tool for electric power systems with a high penetration of electronic power converters. Electr. Power Syst. Res. 210(1), 108–115 (2022)
6. Kundur, P., Paserba, J., Ajjarapu, V., Andersson, G., Bose, A., Canizares, C., et al.: Definition and classification of power system stability ieee/cigre joint task force on stability terms and definitions. IEEE Trans. Power Syst. 19(3), 1387–1401 (2004)
7. Hatziargyriou, N., Milanovic, J., Rahmann, C., Ajjarapu, V., Canizares, C., Erlich, I., et al.: Definition and classification of power system stability–revisited & extended. IEEE Trans. Power Syst. 36(4), 3271–3281 (2020)
8. Sanchez Gasca, J.J., Vittal, V., Gibbard, M., Messina, A., Vowles, D., Liu, S., et al.: Inclusion of higher order terms for small-signal (modal) analysis: committee report-task force on assessing the need to include higher order terms for small-signal (modal) analysis. IEEE Trans. Power Syst. 20(4), 1886–1904 (2005)
9. Zhang, H., Wang, X., Harnefors, L., Gong, H., Hasler, J.P., Nee, H.P.: Siso transfer functions for stability analysis of grid-connected voltage-source converters. IEEE Trans. Ind. Appl. 55(3), 2931–2941 (2019)
10. Raza, M., Prieto Araujo, E., Gomis Bellmunt, O.: Small-signal stability analysis of offshore ac network having multiple vsc-hvdc systems. IEEE Trans. Power Delivery 33(2), 830–839 (2017)
11. Odun Ayo, T., Crow, M.L.: Structure-preserved power system transient stability using stochastic energy functions. IEEE Trans. Power Syst. 27(3), 1450–1458 (2012)
12. Bosetti, H., Khan, S.: Transient stability in oscillating multi-machine systems using lyapunov vectors. IEEE Trans. Power Syst. 33(2), 2078–2086 (2017)
13. Vu, T.L., Turitsyn, K.: Lyapunov functions family approach to transient stability assessment. IEEE Trans. Power Syst. 31(2), 1269–1277 (2015)
14. Pavella, M., Murthy, P.: Transient stability of power systems: theory and practice. John Wiley and Sons, New York, NY (United States), (1994)
15. G D Byrne, A.C.H.: A polyalgorithm for the numerical solution of ordinary differential equations. ACM Trans. Math. Software 1(1), 71–96 (1975)
16. Karawita, C., Annakkage, U.: A hybrid network model for small signal stability analysis of power systems. IEEE Trans. Power Syst. 25(1), 443–451 (2009)
17. Khodaparast, J., Fosso, O.B., Molinas, M., Suul, J.A.: Stability analysis of a virtual synchronous machine-based hvdc link by gear's method. In: I6th IEEE International Energy Conference (ENERGYCon) 1(1), pp. 749–754. IEEE, Piscataway (2020)
18. Fosso, O.B.: Implementation of an implicit method for numerical integration of differential equations with self adaptive time step (Gear's method). NTNU (1993)

19. Stubbe, M., Bihain, A., Deuse, J., Baader, J.: Stag-a new unified software program for the study of the dynamic behaviour of electrical power systems. IEEE Trans. Power Syst. 4(1), 129–138 (1989)
20. Kuijstermans, F.C.M.: Design of nonlinear circuits: The linear time-varying approach. Doctoral Thesis, Delft University of Technology (2004)
21. Van Der Kloet, P., Neerhoff, F.: Behaviour of dynamic eigenpairs in slowly-varying systems. NDES 99(1), 15–17 (1999)
22. Wu, M., Sherif, A.: On explicit solution, stability, and reduction of a class of linear time-varying discrete-time systems. Int. J. Control 25(2), 303–310 (1977)
23. van der Kloet, P., Neerhoff, F., de Anda, M.: The dynamic characteristic equation. NDES 99(1), 77–80 (2002)
24. Dasgupta, S., Paramasivam, M., Vaidya, U., Ajjarapu, V.: Real-time monitoring of short-term voltage stability using pmu data. IEEE Trans. Power Syst. 28(4), 3702–3711 (2013)
25. Rüeger, C., Dobrowolski, J., Korba, P., Sevilla, F.R.S.: IEEE. Lyapunov exponent for evaluation and ranking of the severity of grid events on extra-large power systems. In: IEEE PES Innovative Smart Grid Technologies Europe (ISGT-Europe), vol. 1(1), pp. 1–5. IEEE, Piscataway (2019)
26. Kundur, P., Balu, N.J., Lauby, M.G.: Power System Stability and Control. McGraw-hill New York (1994)
27. Anderson, P.M., Fouad, A.A.: Power System Control and Stability. John Wiley & Sons, Hoboken (2008)
28. Saadat, H., et al.: Power System Analysis. McGraw-Hill, New York (1999)
29. Shen, L.: Model integration and control interaction analysis of AC/VSC HVDC system. Doctoral Thesis, The University of Manchester (2015)
30. Amin, M., Suul, J., D'Arco, S., Tedeschi, E., Molinas, M.: Impact of state-space modelling fidelity on the small-signal dynamics of vsc-hvdc systems. In: 11th IET International Conference on AC and DC Power Transmission, vol. 1(1), pp. 1–11. IET, Stevenage (2015)

How to cite this article: Khodaparast, J., Fosso, O.B., Molinas, M., Suul, J.A.: Static and dynamic eigenvalues in unified stability studies. IET Gener. Transm. Distrib. 1–15 (2022). https://doi.org/10.1049/gtd2.12547